ROYAL SOCIETY
OF CHEMISTRY

FEATURE ARTICLE

The quest for optical magnetism: from split-ring resonators to plasmonic nanoparticles and nanoclusters

Francesco Monticone and Andrea Alù*

Natural materials exhibit negligible magnetism at optical frequencies, since the direct effects of the optical magnetic field on matter are much weaker than electric ones. In the last decades, however, scientists and engineers have been trying to tackle and overcome these limitations by designing artificial subwavelength meta-molecules that support a strong magnetic response, even if made of non-magnetic materials. These issues have become popular because of the excitement around magnetic metamaterials and their exotic wave interaction. Here, we review recent efforts on this topic, with particular focus on magnetic metamaterials operating at optical frequencies. We discuss how the concept of split-ring resonators, introduced at microwaves to realize artificial magnetic inclusions with subwavelength footprint, can be translated to the optical region exploiting the plasmonic features of metallic nanoparticles suitably arranged in nanoclusters and nanorings. We also show that Fano interference effects, triggered by small symmetry-breaking in nanoclusters, may be the key to largely boost the magnetic response in optical meta-molecules. All these findings show that the alliance of optical metamaterials and advanced nanotechnology holds the promise to provide significant advances in the quest towards low-loss optical magnetic materials.

1. Introduction

Nature exhibits a universal lack of symmetry between electric and magnetic charges. The former are ubiquitous and represent the basis of a large number of natural phenomena, while the latter, although allowed in principle, are unstable in reality, a fundamental consequence of the small value of the Sommerfeld fine-structure constant α.[1,2] Interestingly, if the constant were larger than unity, this asymmetry would be reversed and magnetic monopoles would be stable and abundant,[1] but the universe would look fundamentally different.

Department of Electrical and Computer Engineering, The University of Texas at Austin, 1 University Station C0803, Austin, Texas 78712, USA. E-mail: alu@mail.utexas.edu

Francesco Monticone is a graduate research assistant in the Metamaterials and Plasmonics Research Laboratory of Dr Andrea Alù at The University of Texas at Austin, where he is currently pursuing a Ph.D. in Electrical and Computer Engineering. He previously received a B.Sc (2009) and M.Sc. degree (2011) from Politecnico di Torino, Italy. His research work on optical metamaterials, meta-surfaces and plasmonics has been published in top-tier journals, including Physical Review Letters, Nature Nanotechnology, and Science. He has been awarded the Best Student Paper Award at the Metamaterials'2013 conference, an IEEE AP-S Doctoral Research Award, and the H.L. Bruce Graduate Fellowship.

Andrea Alù is an Associate Professor and the David & Doris Lybarger Endowed Faculty Fellow in Engineering at the University of Texas at Austin. He received the Laurea (2001), MS (2003) and PhD (2007) degrees from the University of Roma Tre, Rome, Italy. His research interests span over a broad range of technical areas, including applied electromagnetics, nano-optics, nanophotonics, and acoustics. He is the co-author of an edited book on optical antennas and over 250 journal papers. Dr Alù has received several awards, including the OSA Adolph Lomb Medal (2013), and the URSI Issac Koga Gold Medal (2011). He is a Fellow of OSA and IEEE and an IEEE AP-S Distinguished Lecturer.

In nature, while electrical field lines emerge and terminate on electric charges, magnetic fields are always solenoidal, as there are no single magnetic charges from where the magnetic field lines diverge or converge. In fact, natural magnetism in matter does not originate from magnetic charges, but rather from[3,4] (a) electrical currents, such as orbital currents in atoms, or circulating eddy currents sustained by conduction electrons, or (b) magnetic dipole moments of subatomic particles, due to their intrinsic angular momentum or "spin", whose alignment under an applied magnetic field can produce strong paramagnetic response.

The natural weakness of magnetism at optical frequencies is fundamentally associated to the mentioned asymmetry between electric and magnetic effects. In fact, direct coupling of the magnetic field with a single atom (proportional to the Bohr magneton[3,5]) is $\alpha^{-1} \approx 137$ times weaker than electric coupling. Moreover, due to the absence of free magnetic monopoles, magnetic-based plasmonic properties are not available in natural materials. The very physical meaning of magnetization and magnetic susceptibility in matter has even been questioned for electromagnetic fields at sufficiently high frequencies, as a magnetic polarizability cannot be meaningfully associated to the response of materials at these frequencies.[4,6] This is also related to the fact that, at any frequency, Maxwell's equations can be written embedding the magnetic polarization into a proper spatial dispersion of the electric permittivity ε,[4] implying that specific forms of spatial dispersion of ε produce effects that are not distinguishable from those of a non-unitary magnetic permeability μ. While at lower frequencies it makes sense to define a local permeability different than unity, at higher frequencies magnetism is often comparable or weaker than other forms of spatial dispersion.[7] In light of these considerations, we may envision that, although magnetism in its conventional sense may not be available at high frequencies, it may be possible to properly tailor spatial dispersion and nonlocal electric effects in such a way to induce a noticeable magnetic dipole moment without other higher-order contributions, even though the involved materials do not present microscopic magnetization and their magnetic permeability is strictly unitary.

The magnetic response of natural materials starts to tail off at relatively low frequencies, already in the GHz range. Some ferrites and superconductors still exhibit noticeable ferromagnetism and diamagnetism, respectively, up to the low THz range; however, these materials are generally bulky, or require conditions not suitable for most applications, such as the very low temperatures required by superconductors, or the limitations dictated by their not ideal mechanical properties. Therefore, the search for alternative approaches to magnetism and boosted or tunable magnetic response has been an active topic of research for a few decades in the GHz range and beyond. This has been one the main motivations behind the development of artificial magnetic structures at microwave frequencies, such as split-ring resonators (SRRs), originally proposed in the 1940s[8] and seminally applied by Pendry to metamaterials.[9]

These structures, despite their subwavelength footprint, exhibit strong magnetic dipole moments, although based on non-magnetic (or weakly diamagnetic) materials, and are therefore ideal to induce strong average magnetization in microwave composite materials. In fact, a dense array of such subwavelength structures responds to electromagnetic waves as an effective homogeneous medium, with "emergent" material properties that can become drastically different from those of its constituents. In such an engineered material, or metamaterial, the effective magnetic permeability and electric permittivity are not uniquely determined by the chemical composition of the materials involved, but also by the engineered structure and arrangement of its inclusions. Since natural atoms and molecules do not provide an individually strong electromagnetic response, they typically do not offer large flexibility in the design of magnetic materials; however, the metamaterial paradigm has proven to be particularly useful in this context. Indeed, the possibility of realizing strong effective magnetic response by tailoring artificial meta-atoms and meta-molecules has been one of the main triggers for the explosion of interest in metamaterials in the last decade, building on earlier investigations on artificial dielectrics and complex media, e.g., ref. 10 and 11. By overcoming the limited magnetic properties of naturally occurring materials, metamaterials have opened a world of new possibilities, often thought impossible only a few decades ago, such as the realization of strong artificial diamagnetism ($\mu \approx 0$) and paramagnetism ($\mu > 1$) at frequencies above the GHz range, or negative permeability and negative refraction, which are at the basis of perfect lenses,[12] miniaturized antennas,[13] invisibility cloaks,[14] among many other fascinating examples (see, e.g., ref. 11 and 15 and references therein).

The realization of artificial and anomalous magnetism, already exciting in the radio-frequency and microwave range, becomes of fundamental scientific significance at infrared and optical frequencies, where no natural material offers noticeable magnetic response. Magnetic metamaterials at microwaves are generally based on different forms of conducting meta-atoms (usually variations of the SRR geometry), with subwavelength dimensions in the order of the millimeters. Translating these concepts above the THz range, however, has proven very challenging, as we discuss in the next section. In this feature article, we present recent research efforts aimed at attaining artificial magnetism in the optical range. Particular attention will be devoted to optical metamaterials based on plasmonic nanoparticles and nanoclusters, and to how they may lead to strong magnetic response at high frequencies. In the interdisciplinary spirit of the field of metamaterials, we will draw relevant connections and analogies with the fields of chemistry (hybridization and group theory of plasmonic modes) and electrical engineering (lumped circuit elements and resonators), which provide deep physical insights into the involved phenomena through simple and intuitive models. In the last section, we will also present our recent theoretical and experimental investigations on asymmetric rings of plasmonic nanoparticles, which realize strong artificial magnetism in the visible range and can enhance magnetic light-matter interactions at the nanoscale.

9060 | J. Mater. Chem. C, 2014, **2**, 9059–9072

This journal is © The Royal Society of Chemistry 2014

2. From split-ring resonators to plasmonic nanoparticles

Any conductor exhibits a moderate diamagnetism, since an impinging time-varying magnetic field induces circular currents that, according to Lenz's law, flow in a direction that opposes any change in the magnetic flux;[3] as a result, the induced magnetic moments are directed opposite with respect to the incident magnetic field. This natural diamagnetism in conductors, however, is generally weak and often hidden by other paramagnetic effects, so that the overall magnetic response of real conductors at room temperatures is almost negligible. To achieve stronger magnetism, conducting materials may be shaped in order to properly guide the induced conduction current, producing a resonant circulating current flow when illuminated by an oscillating magnetic field. SRRs are purposely designed to obtain this resonant response at a sub-wavelength scale (Fig. 1a): the inductive response of a metallic ring is combined with the capacitance introduced by a small gap in the ring, where conduction electrons can accumulate and be depleted at each cycle. The overall subwavelength structure acts as a lumped inductor–capacitor (LC) resonator (inset of Fig. 1a) and supports a strong magnetic dipole moment **m** normal to the plane of the ring.

$$\mathbf{m} = \frac{1}{2} \int_V \mathbf{r} \times \mathbf{J} \, dV, \tag{1}$$

where **J** is the current flowing in the SRR, V is the unit cell volume and **r** is the position vector from the center of the ring. In many cases, in order to increase the capacitance of the meta-atom, a second concentric split ring is introduced with opposite gap (as in the inclusions of the metamaterial in Fig. 1b). This also improves the "purity" of the magnetic response by minimizing the electric dipole moment associated with the charge separation at the gaps. As we will see in the following, an analogous issue arises at optical frequencies, where the weak magnetic response sustained by meta-atoms is generally over-shadowed by stronger electric resonances. Throughout this paper, emphasis is placed on the "purity" of the magnetic response, indicating the comparison in terms of scattered power between the magnetic contribution and the induced electric dipole moment and other multipolar terms (typically the electric quadrupole moment). Higher purity implies that the magnetic response dominates over these other contributions.

SRRs have been successfully used as magnetic meta-atoms for several applications in the microwave range, including the first experimental demonstration of negative index of refraction[16,17] (Fig. 1b), fulfilling the speculations and predictions made by Veselago in 1967 on the electromagnetic response of materials with simultaneously negative ε and μ.[18,19] Given the success of SRRs, and their analogues, at microwave frequencies, several research groups started investigating the possibility to scale these concepts at higher frequencies. The frequency of the magnetic resonance in SRRs can be approximately evaluated from its equivalent LC circuit model as $\omega_m = 1/\sqrt{LC}$. For the square SRR geometry in Fig. 1a, the inductance of the conducting ring is $L = \mu_0 l^2/t$ and the gap capacitance $C = \varepsilon_0 wt/d$, where μ_0 and ε_0 are the magnetic permeability and electric permittivity of free space, respectively, l is the length of the SRR side, t the metal thickness, w its width and d the gap size. This simple circuit model reveals, qualitatively, that the resonance frequency is inversely proportional to the size A of the SRR, assuming all the dimensions scale proportionally with A,[5,21,22]

$$\omega_m = c_0 \sqrt{d/wl^2} \propto 1/A, \tag{2}$$

where c_0 is the speed of light in vacuum. By shrinking the dimensions of the unit cell, the magnetic resonance will shift to higher frequencies, as intuitively expected (similar considerations apply also to double SRRs). Based on this scaling rule, the artificial magnetic response of metamaterials has been pushed into the low THz region, as demonstrated in ref. 23 using scaled SRRs fabricated with photolithographic techniques (Fig. 2a). However, at even higher frequencies, a mere scaling of these meta-atoms is not sufficient, due to changes in the conduction properties of metals. From the THz region upward, in fact, metals can no longer be modeled as dispersionless perfect conductors; instead, their finite carrier density causes the electrons to react to the electromagnetic excitation with increasing time delay, resulting in a frequency dispersive permittivity and a finite plasma frequency. The increased electron inertia corresponds to significant kinetic inductance L_{kin} that can no longer be neglected in the material response. In particular, it has been shown that the additional kinetic inductance of a metallic ring scales inversely with the unit cell size A,[21,22] hence dominating the response for small SRRs. As a result, the magnetic resonance frequency becomes

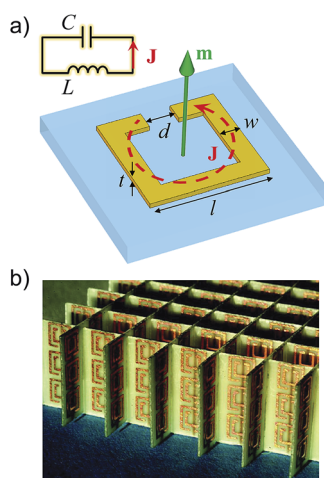$$\omega_m = \sqrt{(L + L_{kin})C} \propto 1/\sqrt{A^2 + \text{const.}}, \tag{3}$$

Fig. 1 Magnetic metamaterials at microwave frequencies. (a) Schematic of a single SRR as a magnetic meta-atom. The resonant circulating current **J** supports a magnetic dipole moment **m** normal to the ring plane. The inset shows the equivalent lumped circuit model of the SRR. (b) Negative-index metamaterials composed of double SRRs and wires. From ref. 17 reprinted with permission from AAAS.
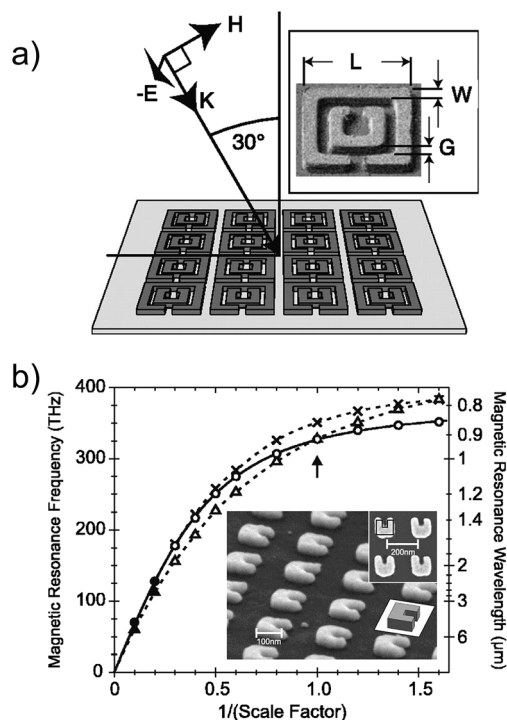
Fig. 2 (a) THz metamaterials based on scaled double SRRs, fabricated with photolithographic techniques. The dimension of the unit cell is in the order of tens of micrometers, resulting in a magnetic resonance around 1 THz. The magnetic response is obtained at oblique incidence. From ref. 23 reprinted with permission from AAAS. (b) Scaling behavior of the magnetic resonance of SRRs in the infrared range. The different symbols indicate different cases studied numerically (see ref. 22 for details), whereas the solid line corresponds to a fit using the LC model in eqn (3). The arrow denotes the position of the weak electrically-coupled magnetic resonance of the U-shaped SRRs shown in the inset. Adapted with permission from ref. 22.

which saturates to a maximum value in the near-infrared region[21,22] when the size of the meta-atom vanishes, as shown in Fig. 2b. Different circuit models for SRRs consistently predict similar saturation frequencies.[21,22,24]

Several variations on the original SRR design have been proposed to extend its functionality to the THz range and beyond. For example, weak magnetism has been demonstrated in the mid- and near-infrared range using electrically-coupled single SRRs,[22,25,26] in which the electric field induces a weak magnetic moment when it is normal to the plates of the gap capacitance. Other variations include arrays of metallic "nano-staples"[27] vertically mounted above a metallic mirror (from which they are separated by a dielectric spacer that introduces a gap capacitance), and metallic rings with multiple gaps,[21,28,29] whose magnetic resonance has been shown to saturate at higher frequencies compared to single-gap SRRs.[21] However, it has become increasingly clear that the SRR geometry cannot provide strong magnetism and negative permeability above 100 THz, and especially in the visible range. To overcome these limitations, a variety of different ideas have been also proposed to attain artificial magnetism and negative refraction at higher frequencies. For example, an interesting possibility is offered by

the natural Mie resonances in dielectric particles with high permittivity.[30–33] For dielectric spherical particles with refractive index larger than about two,[33] the dominant Mie scattering resonance is a magnetic dipole resonance occurring when the wavelength inside the particle is approximately equal to the sphere diameter. By arranging these particles in large dense arrays, it is then possible to realize all-dielectric metamaterials with a strong magnetic response, even characterized by a negative effective permeability at optical frequencies.[30–32] This approach has the advantages of reduced material losses, compared to metallic optical metamaterials, and the fact of being based on simple building blocks, arguably easier to fabricate than SRRs at optical frequencies. An important limitation of these structures, however, is related to the limited dielectric response of natural materials at optical frequencies (the highest optical refractive index is only about four, in silicon and germanium), which poses a fundamental limit to the scaling of the resonant dielectric meta-atoms towards smaller sizes. For similar reasons, Mie resonances in dielectric particles do not exhibit the often-desirable strong near-field enhancement that characterizes, instead, plasmonic resonances in small metallic structures. In Section 4, we will discuss how metallic inclusions may lead to strong magnetic hot spots in the near field, potentially useful in different scenarios.

Other interesting solutions to achieve artificial magnetism at optical frequencies include electrostatic resonances in sub-wavelength periodic nanostructures,[34–36] dielectric and metallic photonic crystals,[37–40] and closely coupled plasmonic elements, e.g., nanowires, nanostrips, nanospheres.[41–50] Notably, in this latter category, the onset of plasmonic effects in metals at optical frequencies, which hinders the scalability of SRRs, is exploited advantageously to guide the displacement current flow and sustain subdiffractive magnetic resonances. At sufficiently high frequency, in fact, while the conduction current is weakened, the displacement current $\mathbf{J}_d = -i\omega\mathbf{D}$, namely, the time-derivative of the electric displacement $\mathbf{D}$ (under a time-harmonic excitation $e^{-i\omega t}$), becomes dominant. Therefore, it appears possible to realize a strong magnetic moment even in the optical range by designing engineered plasmonic meta-atoms in which the displacement current takes the role of conduction current in low-frequency SRRs. As an example, coupled metallic nanorods and nanostrips (Fig. 3a and b) have been designed to support anti-symmetric resonant modes with a noticeable magnetic contribution, as seen in Fig. 3c. These geometries have been successfully exploited to demonstrate negative permeability throughout the visible range[45] (Fig. 3d). Besides, when combined with metallic strips oriented along the incident electric field, the resulting "fishnet" structure allows the realization of an effective negative index of refraction in the optical range.[51–53]

All these metamaterials based on paired plasmonic elements, however, have rather weak and non-ideal magnetic responses. In fact, as discussed in ref. 47, in any plasmonic meta-molecule formed by two coupled elements, the magnetic resonance associated with the anti-symmetric mode is always accompanied by electric-quadrupole radiation and other higher-order multipoles, which lead to increased radiation

9062 | J. Mater. Chem. C, 2014, **2**, 9059–9072

This journal is © The Royal Society of Chemistry 2014
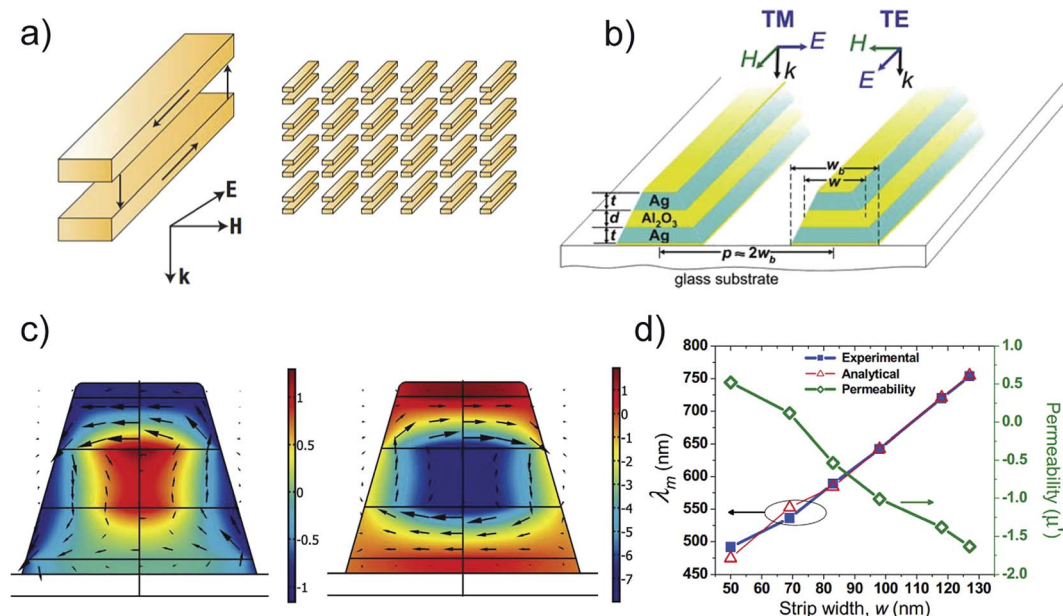
Fig. 3 (a) Paired nanorods and (b) nanostrips supporting a magnetic resonance associated with the anti-symmetric mode. Adapted with permission from ref. 5 and 44, respectively. (c) Simulated magnetic field (colors) and electric displacement (arrows), at the electric (left) and magnetic (right) resonances, for the geometry in (b) under transverse-magnetic (TM) illumination (note the different color scales in the two panels). Reproduced with permission from ref. 45. (d) Effective magnetic permeability and magnetic resonance frequency as a function of the average width of the trapezoidal geometry in (b). Reproduced with permission from ref. 45.

losses and non-negligible spatial dispersion in the meta-material response. In order to achieve a "purer" magnetic response in the visible range, the number of plasmonic elements that guide the displacement current in the meta-molecule needs to be increased. Notably, particularly strong optical magnetism has been obtained with nanorings formed by nanospheres arranged in a subwavelength loop,[46–48] as depicted in Fig. 4a. In this structure, the plasmonic oscillations of the nanospheres and their tight coupling guide the displacement current in a resonant circulating flow, producing a strong magnetic dipole moment normal to the plane of the ring. As we

discuss in the next section, such plasmonic nanorings may be described as lumped resonant circuits for the displacement current, hence transplanting the SRR concept to optical frequencies.

3. Artificial optical magnetism using plasmonic nanorings and nanoclusters

3.1 Theory of artificial optical magnetism based on nanoparticle rings

Plasmonic nanoparticles (NPs) have been extensively used as basic building blocks for optical metamaterials and meta-surfaces (see, e.g., ref. 54 and references therein). Plasmonics, in fact, offers an ideal solution to the problem of realizing deeply subwavelength optical resonators, thanks to the strong coupling of incident photons with collective oscillations of the electron gas, i.e., plasmons, which determines highly localized and enhanced fields and largely reduced resonance length.[55] Plasmonic materials, such as noble metals in the visible range,[55] aluminum at UV frequencies[56,57] and highly-doped semi-conductors in the infrared region,[58,59] have been successfully exploited to realize extreme forms of light-matter interaction and anomalous scattering effects. The optical response of plasmonic NPs and their quasi-static resonances, in fact, can be largely tuned by changing their shape, or considering multiple layers made of different dielectric and plasmonic materials. A number of useful and intriguing optical effects have been demonstrated based on engineered plasmonic NPs, including ultra-sharp Fano resonances,[60–62] plasmon-induced transparency,[63] light-trapping by embedded photonic
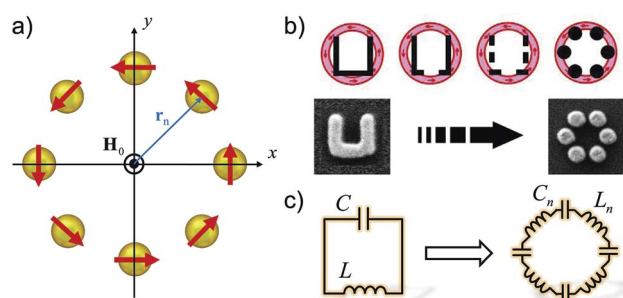
Fig. 4 (a) Schematic of a symmetric ring of plasmonic NPs excited by a uniform magnetic field H_0 normal to the plane. The red arrows represent the circulating electric dipole moments that support the magnetic response of the structure. (b) Illustrative evolution of magnetic meta-atoms, from a SRR geometry to a ring of plasmonic NPs. Reproduced with permission from ref. 76. (c) Corresponding equivalent circuit evolution, showing that both SRRs and nanorings can be interpreted as lumped LC resonators.

eigenvalues,[64,65] invisibility and cloaking,[66,67] as well as enhanced non-linear response and optical bistability.[68,69]

In the relevant case of spherical (single or multi-layered) particles, the optical response can be calculated exactly, applying the rigorous Mie solution of Maxwell's equations.[70] For more complicated scenarios, however, it is often convenient to resort to approximate techniques that simplify the design and analysis of the considered nanostructures, while still capturing the relevant phenomena. For example, in the quasi-static regime, the optical response can be suitably modularized by treating the nanoelements as optical nanocircuits or nano-antennas,[69,71,72,73] in analogy with their low-frequency counterparts. In this context, the optical impedance of a NP can be defined as the ratio of the local potential difference and the flux of displacement current through the NP, yielding $Z_{opt} = il/(\omega\varepsilon_0\varepsilon S)$, where l is the length of the NP along the local electric field, S its transverse cross-section and ε its relative permittivity. The so defined optical impedance is an intrinsic property of the NP, independent of the surrounding environment. This way, the design and analysis of plasmonic nanostructures can be carried out, at least qualitatively, with simple and elegant rules borrowed from circuit theory and microwave engineering, avoiding the need for solving a full-wave electromagnetic problem every time, particularly convenient in multi-particle systems,[73] or when NPs are coupled to optical waveguides, quantum emitters, or nanoantennas.[74] This optical nanocircuit paradigm provides useful physical insights into light–matter interactions at the nanoscale, and allows drawing relevant connections with analogous phenomena at lower frequencies.

As discussed at the end of Section 2, engineered rings of plasmonic NPs (Fig. 4a) have been shown to realize strong magnetic dipole response in the near-infrared and visible regions.[46–48] Interestingly, in light of the nanocircuit paradigm described above, such subwavelength nanorings can be seen as the resonant interconnection of optical nanoinductors (the plasmonic NPs) and nanocapacitors (the insulating air gaps), given their opposite real parts of permittivity, arranged in a loop configuration.[47,75] This interpretation indicates that plasmonic nanorings can be considered the optical equivalent of low-frequency SRRs, in which inductor–capacitor pairs have been "distributed" along the entire loop (see Fig. 4b and c) in order to better guide the circulating flow of displacement current. Despite these relevant analogies, the plasmonic features of such meta-molecules determine important differences compared to their longer-wavelength counterparts, enriching this area of research with novel possibilities. A notable difference is the fact that, while in a conventional conducting SRR the resonance frequency is inversely proportional to the ring size, as we showed in Section 2, in a plasmonic nanoring the magnetic resonance is only weakly related to the size of the unit cell, whereas it mainly depends on the plasmonic resonances of the single NPs.[46,47] In fact, in the ring geometry shown in Fig. 4, the optical inductance of each plasmonic NP is a property of the particle itself, independent of the arrangement of the other particles and the ring size. As a result, if we shrink the radius of the nanoring, keeping the same particles, the magnetic resonance will actually shift to longer wavelengths, as the

capacitance will increase due to smaller inter-particle gaps, while the inductance remains essentially the same. Therefore, it is possible to realize deeply subwavelength meta-molecules with a magnetic resonance at the desired frequency, determined by the properties of each NP (its shape and composition) and the size of the capacitive gaps between them.

Although the simple and intuitive interpretation based on optical nanocircuits provides useful physical insight, a more rigorous analysis of plasmonic nanorings is necessary to quantitatively assess their magnetic properties. Owing to the small size of the NPs compared to wavelength, and assuming that neighboring NPs are not extremely close, the interaction among the different spheres composing the nanoring can be described, in first approximation, by their induced electric dipole moments $\mathbf{p}_n = \alpha\mathbf{E}_{loc}(\mathbf{r}_n)$, where α is the electric dipole polarizability of the NPs (assumed non-magnetic) and $\mathbf{E}_{loc}(\mathbf{r}_n)$ is the local electric field at the location $\mathbf{r}_n$ of the n-th sphere, determined by the incident electric field and the fields reradiated by all other NPs. For a homogeneous and isotropic sphere the polarizability is a scalar and it can be conveniently written as

$$\alpha^{-1} = \left(4\pi\varepsilon_0 a^3 \frac{\varepsilon - \varepsilon_0}{\varepsilon + 2\varepsilon_0}\right)^{-1} - i\frac{k_0^3}{6\pi\varepsilon_0}, \qquad (4)$$

where a is the radius of the NP, ε its relative permittivity and k_0 is the free-space wavenumber. For lossless objects, the imaginary part of the inverse polarizability is independent of the properties of the particle and corresponds to the local photonic density of states, related to the radiation loss of the particles. Following the derivation in ref. 46, after properly considering the electric dipolar interaction among the NPs, the magnetic polarizability of the nanoring can be analytically written as

$$\alpha_m^{-1} = \frac{4\varepsilon_0}{Nk_0^2 R^2}\alpha^{-1} - \frac{1}{16\pi Nk_0^2 R^5}\sum_{l\neq n}^{N}\frac{3 + \cos[2\pi(l-n)/N]}{|\sin[\pi(l-n)/N]|^3}$$
$$- i\left(\frac{k_0^3}{6\pi} - \frac{2k_0}{3\pi NR^2}\right), \qquad (5)$$

where N is the number of particles and R the radius of the nanoring (assumed to be electrically small, i.e., $k_0 R \ll 2\pi$). Comparing eqn (4) and (5), it is possible to verify that the magnetic resonance frequency of the nanoring is mainly determined by the plasmonic resonance of the individual NPs (occurring at frequencies for which $\mathrm{Re}[\varepsilon] \approx -2\varepsilon_0$), moderately shifted by the coupling between NPs [the summation terms in eqn (5)]. Interestingly, this is consistent with our qualitative discussion based on lumped optical nanocircuits, confirming that the magnetic resonance of plasmonic nanorings is not mainly caused by the size of the unit cell, as it is instead for conventional SRRs. Further power considerations and a full-dynamic analysis of plasmonic nanorings are discussed in ref. 47.

In order to realize a magnetic metamaterial at optical frequencies, the subwavelength nanoring inclusions are then arranged in large three-dimensional arrays, whose effective material properties can be obtained by applying appropriate mixing rules and homogenizing formulas.[77,78] For example, for an infinite three-dimensional cubic lattice, Clausius–Mossotti homogenization gives the relative magnetic permeability as

9064 | J. Mater. Chem. C, 2014, **2**, 9059–9072

This journal is © The Royal Society of Chemistry 2014

$$\mu_{\text{eff}} = 1 + \frac{N_d}{\alpha_m{}^{-1} + i\left(k_0{}^3/6\pi\right) - N_d/3}, \qquad (6)$$

where N_d is the number density of inclusions per unit volume and the magnetic polarizability of the meta-molecule α_m is given by eqn (5). It is important to stress that, while the radiation losses due to the magnetic dipole of each nanoring are compensated by the periodicity of the lattice [the imaginary term at the denominator of eqn (6), in fact, would not be present in a random array], the radiation losses associated with spurious higher-order multipoles may in general contribute to the imaginary part of the effective magnetic permeability in this simple model. Therefore, even in the case of lossless inclusions, the metamaterial may exhibit a non-zero imaginary part of μ_{eff} due to such residual radiation losses. In Fig. 5a, we show the calculated dispersion of the effective permeability for different number of particles composing the nanoring inclusions. It is evident that strong diamagnetism, paramagnetism and negative permeability are obtained around the magnetic resonance in the visible range. Besides, a larger number of particles strengthens the magnetic response, while the resonance frequency is red-shifted due to increased coupling among NPs. Notably, the case with only two nanoparticles exhibits modest artificial magnetism, associated with the anti-symmetric resonance of the pair, but the response is strongly damped by ohmic and radiation losses.

We reiterate that the strong optical magnetism demonstrated in Fig. 5a is based on purely non-magnetic materials (the magnetic polarizability of the NPs is zero), a fact that is not in contradiction with Landau's argument about the magnetic susceptibility at optical frequencies,[4] as discussed in the Introduction. Here, the resonant magnetic response of the meta-molecule is sustained by the displacement current, guided in a circular loop by the plasmonic resonances of the NPs, as shown in the full-wave simulation in Fig. 5b. This mechanism yields an arguably stronger and "purer" magnetic dipole moment compared to other available solutions for magnetic materials at visible frequencies. Moreover, the electric response of the nanoring can also be engineered in order to have an electric dipole resonance spectrally overlapped with the

magnetic one. As a result, negative effective permittivity and permeability can be obtained in the same frequency window, thereby synthesizing a negative-refractive-index metamaterial in the visible range.[46,47]

The scalar magnetic polarizability in (5) is valid for the specific illumination considered here (namely, a magnetic field normal to the ring plane, as sketched in Fig. 4a). In general, however, the planar nanoring is anisotropic and polarization-dependent, with a tensorial magnetic polarizability. Nevertheless, it has been shown that a simple extension of this geometry, using 6 nanoparticles in a symmetric 3D configuration, may effectively realize an isotropic lumped magnetic building block in the visible range,[48] in analogy with 3D arrangements of SRRs at microwaves.[79] Alternatively, spherical constellations of plasmonic NPs surrounding a dielectric core have been shown to support isotropic resonant magnetic response,[80–82] but their moderately large size may determine a large red-shift of the magnetic resonance and the onset of higher-order scattering contributions. Isotropic magnetic inclusions have also been exploited to demonstrate magnetic-based plasmon waves in the visible range,[48] which is particularly exciting as natural magnetic plasmons are not available, due to the absence of free magnetic monopoles in nature.

3.2 Plasmon hybridization model and magnetic nanoclusters

The attractiveness of rings of plasmonic NPs as building blocks for optical magnetic metamaterials has triggered several recent experimental attempts to measure a noticeable magnetic response in plasmonic nanoclusters. The fabrication of such structures can be carried out using top-down processes (e.g., ref. 83), such as electron-beam lithography and focused-ion beam milling, or alternatively, by assembling colloidal NPs in nanoclusters through self-assembly processes,[84–86] or atomic force microscopy (AFM) nanomanipulation.[87–89] The chemical synthesis of colloidal nanospheres,[90] or more complex nanoshells,[91] is well established at the present day and NPs of different materials and dimensions are commercially available from several manufacturers.

A particularly simple and intuitive picture to understand the complex optical response of plasmonic nanoclusters is provided by the "plasmon hybridization model", an electromagnetic analogue of molecular orbital theory.[92–94] When light interacts with an individual plasmonic particle, an electric dipolar plasmon can be excited at a specific wavelength. As different particles are brought into close proximity, their individual plasmons, which correspond to excited clouds of conduction electrons on the surface of the particles, mix and interact, giving rise to hybridized collective modes, analogous to molecular orbitals, as illustrated in Fig. 6a. This intriguing "metachemistry" of plasmonic interactions suggests that, although we may not be able to tailor the orbital currents in natural atoms and molecules, we can engineer meta-molecules and their collective plasmonic modes (or "meta-orbitals") to achieve the desired optical response. For example, a pair of closely-spaced plasmonic particles (nanodimer) supports bonding and antibonding
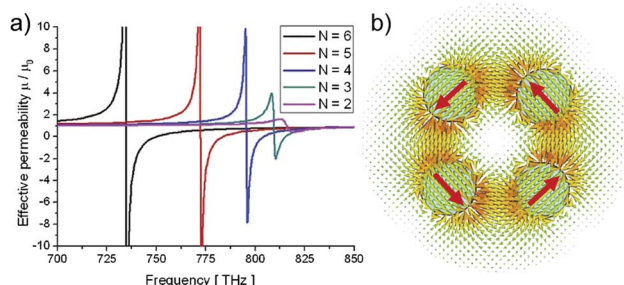

Fig. 5 (a) Real part of the effective permeability of a metamaterial composed of nanoring inclusions as in Fig. 4a, with different number of particles. Reproduced with permission from ref. 47. (b) Time-snapshot of the electric field distribution in a nanoring close to its magnetic resonance. Red arrows represent the electric dipole moments of each particle. Adapted with permission from ref. 46.

This journal is © The Royal Society of Chemistry 2014

J. Mater. Chem. C, 2014, 2, 9059–9072 | 9065
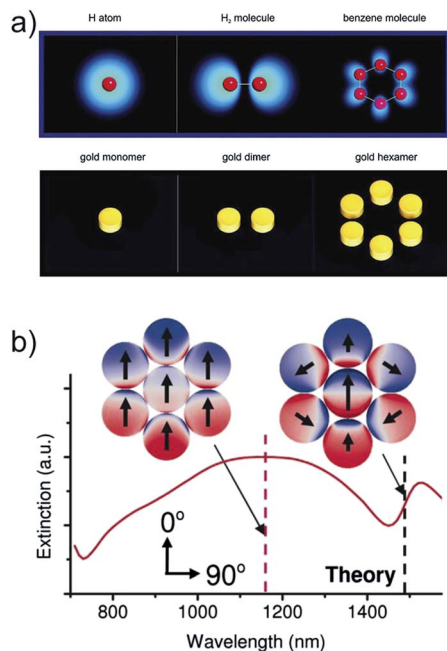
Fig. 6 (a) Analogy between natural molecules and plasmonic nanoclusters, which is at the basis of the hybridization model of plasmonic interactions. Adapted with permission from ref. 83. Copyright 2010 American Chemical Society. In this model, collective plasmonic oscillations in multi-particle clusters originate from the hybridization of individual plasmons, in direct analogy with the hybridization of the electron wavefunctions of individual atoms to form molecular orbitals. (b) Scattering spectrum of a heptamer, showing a pronounced Fano resonance at telecommunication wavelengths. The inset shows the charge density and dipole moment distributions of the bright (left) and dark (right) modes. From ref. 84 reprinted with permission from AAAS.

modes,[93,95] some of which contribute to the weak magnetic response of the pair, as discussed above. Even more interesting optical responses can be obtained with nanoclusters composed of several particles, for example the hexamer in Fig. 6a. It has been shown that, by adding a particle at the center of the hexamer, the collective plasmonic oscillations of the overall nanocluster can be interpreted as the hybridization of the plasmon modes of the 6-particle ring and the central NP.[83] In the resulting bonding mode, all the induced dipole moments of the particles oscillate in phase (left inset of Fig. 6b), along the direction of the incident electric field. This mode strongly couples with farfield radiation, *i.e.*, it is bright, with large radiation damping and reduced lifetime. Conversely, the antibonding mode (right inset of Fig. 6b) is dark, as its radiation efficiency is much lower. Interestingly, these two modes can interfere in the near field, due to their symmetry compatibility,[60,83] giving rise to a strong Fano resonance visible in the farfield scattering spectrum (Fig. 6b). Such Fano resonances generally arise in systems of coupled oscillators with different lifetimes,[96] and are characterized by a peculiar asymmetric lineshape. As we will see in the next section, these interference mechanisms are particularly useful, as a dark mode can be efficiently excited through the coupling with a broader bright mode, resulting in strongly localized and enhanced fields.[60,97]

An interesting attempt to realize a magnetic nanoring is represented by the trimer in Fig. 7a,[84] which synthesizes a closed loop of optical nanoinductors and nanocapacitors, consistent with our discussion in the previous section. The trimer, fabricated through self-assembly of polymer-coated nanoshells, indeed exhibits a magnetic resonance at near-infrared frequencies, as seen in Fig. 7b and c; however, the induced magnetic dipole moment is quite weak, so that a cross-polarizer needs to be used to filter out the dominant electric scattering and "expose" the magnetic resonance (second row Fig. 7c). This is a common problem shared by several experimental attempts aimed at synthesizing magnetic nanorings, as the bright electric resonance is always drastically stronger and, thereby, it tends to shadow the weak magnetic response.[84–86] Since, as discussed in the previous section, the magnetic resonance of the nanoring mainly depends on the electric plasmonic resonances of the individual elements, it does not seem possible to effectively reduce the electric response contribution of the meta-molecule without, at the same time, damping its magnetic moment. Nevertheless, in the next section, we discuss how this issue may be solved with an asymmetric nanoring design, which may advantageously exploit the electric response to boost the magnetic resonance.

## 4. Boosted optical magnetism in asymmetric meta-molecules

The unique capabilities of AFM nanomanipulation allow for active manipulation of NP clusters, offering the possibility to study the evolution of the optical response as the meta-molecule is assembled and modified. In ref. 89, these useful possibilities have been successfully exploited to assemble and characterize a subwavelength nanoring composed of four gold NPs (Fig. 8a and b). Scattering spectra were taken with a dark-field optical microscope during different stages of the meta-molecule assembly. As expected, when the particles are far apart (Fig. 8c and e), the scattering exhibits a single broad peak at around 540 nm, corresponding to the plasmon resonance of individual NPs. Consistent with the discussion in Section 3, when the particles are brought in close proximity, the individual plasmon modes interact with each other producing hybridized collective plasmonic oscillations of the nanocluster. As the distance between the four NPs is reduced, in fact, a large red-shift of the resonance can be observed, due to increased capacitive coupling between neighboring particles. More interestingly, when the NPs are finally assembled in a compact nanoring[98] with small structural asymmetries (Fig. 8d), a pronounced dip in the scattering spectrum is observed (Fig. 8f). As shown in ref. 89, this feature, quite peculiar for such a small nanostructure, is the signature of a Fano interference taking place between the electric and magnetic plasmon modes of the ring, triggered by the asymmetries of the nanocluster.

In general, in symmetric meta-molecules, such as symmetric trimers[84] and quadrumers,[85,86] the magnetic and electric modes are orthogonal and contribute additively to the farfield scattering cross section without interference. This fact can also be

9066 | *J. Mater. Chem. C*, 2014, **2**, 9059–9072

This journal is © The Royal Society of Chemistry 2014
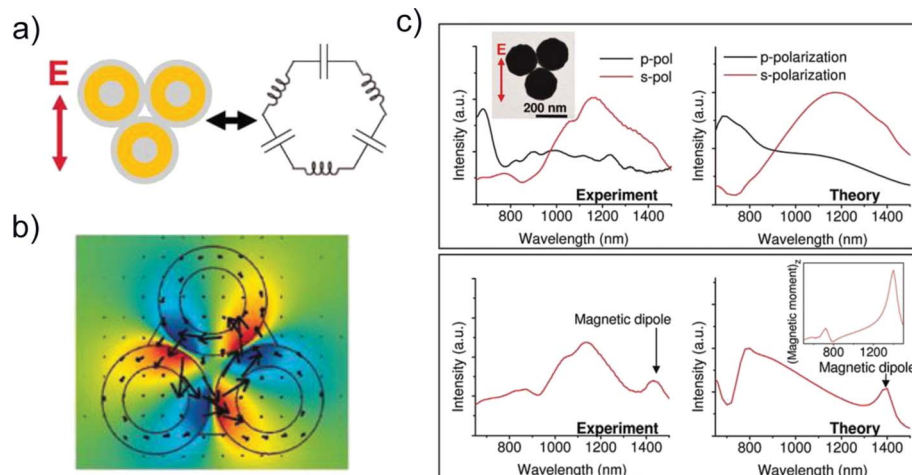
Fig. 7 (a) Schematic of a trimer and corresponding optical circuit model. (b) Distribution of the electric potential (colors) and the displacement field (arrows) at the magnetic resonance of the trimer. (c) Calculated and measured scattering spectra without (top row) and with (bottom row) a cross-polarizer inserted in the collection path. The weak magnetic resonance at infrared frequencies appears only when the bright electric dipole radiation is filtered out by the polarizer. From ref. 84 reprinted with permission from AAAS.
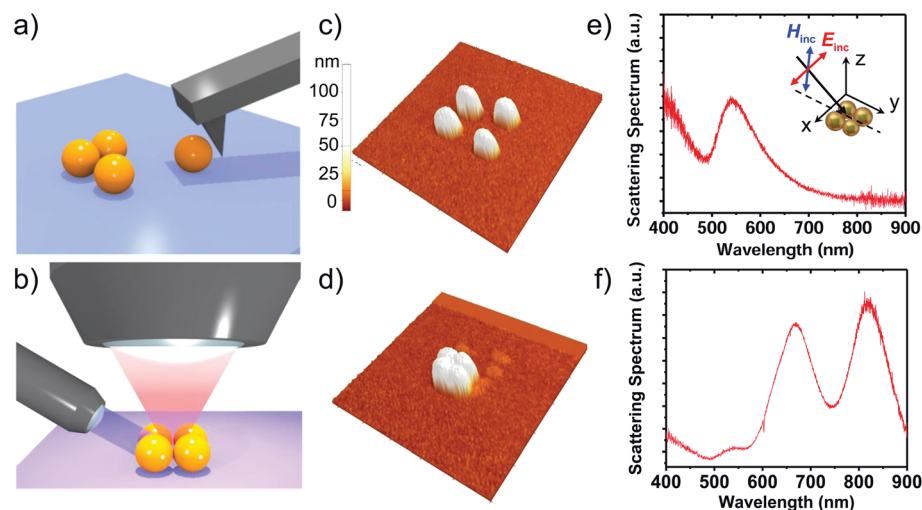
Fig. 8 (a) Illustration of AFM nanomanipulation and (b) optical scattering set-up. (c) and (d) AFM images of a nanoring at two different stages of the nanoassembly process. (e) and (f) Corresponding scattering measurements, demonstrating the dramatic evolution of the scattering response, due to magneto-electric Fano interference in the assembled nanoring. Inset in (e) illustrates the incident polarization. Reproduced with permission from ref. 89.

understood from group theory, which has been used to classify collective plasmon modes into orthogonal irreducible representations according to their symmetries,[60,85] in analogy with natural molecules.[99] In other words, group theory applied to plasmonic meta-molecules defines a set of "selection rules" for mode interaction. For example, in symmetric nanoclusters, the bright electric dipole mode cannot couple with the dark magnetic mode, because they have different irreducible representation.[84,100] However, when small asymmetries are introduced, the modes may lose their orthogonality and their near-field coupling becomes allowed. Therefore, symmetry breaking may induce strong Fano interference effects between electric and magnetic modes in a meta-molecule, creating a characteristic Fano dip in its scattering signature.

By analyzing the simulated polarization distribution in the nanoring of Fig. 8, it is also possible to identify the individual multipolar contributions associated with the measured scattering spectra. As seen in Fig. 9a, in the case of a perfectly symmetric nanoring (dashed lines) the dominant electric dipole response is accompanied, in the same frequency window, by a much weaker magnetic resonance, whereas the electric quadrupole response is almost negligible, thanks to the small size of the ring and the even number of particles, as discussed before. In earlier experimental attempts, instead, the larger size of the nanoclusters (often comparable to the wavelength) caused the magnetic resonance to be substantially red-shifted relative to the electric resonance and to be combined with significant higher-order scattering contributions. The multipole analysis in

This journal is © The Royal Society of Chemistry 2014

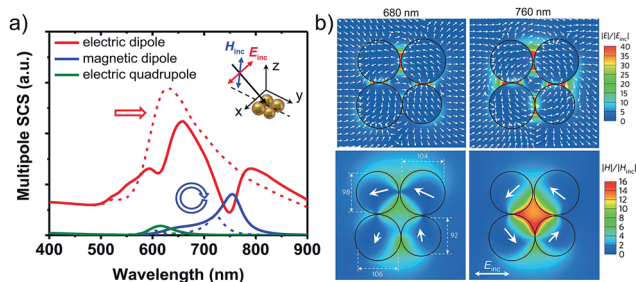*J. Mater. Chem. C*, 2014, **2**, 9059–9072 | **9067**

Fig. 9 (a) Theoretical multipolar analysis of the scattering spectrum for a symmetric (dashed lines) and an asymmetric ring (solid lines), the latter corresponding to the geometry in Fig. 8. The analysis confirms the enhancement of the magnetic response through the coupling with the bright electric resonance. (b, top row) Electric field distribution and field vectors, and (b, bottom row) magnetic field distribution and electric dipole moments at the electric resonance (left panels) and the magnetic resonance (right panels). Adapted with permission from ref. 89.

Fig. 9a confirms that, when small structural asymmetries are introduced in the nanoring, a strong Fano interference occurs between the electric and magnetic plasmon modes. As a result, the magnetic response is significantly boosted from the coupling with the bright electric mode, creating a strong Fano resonance around 760 nm that explains the pronounced dip in the measured scattering spectrum (Fig. 8f). Consistent with our previous discussion, also in the asymmetric case the quadrupole resonance remains significantly weaker than the magnetic response, a very desirable feature for the realization of meta-materials with low radiation losses. These findings represent experimental evidence of a magneto-electric Fano resonance in the visible range.[89,101,102] This effect, stronger than optical Fano resonances based on higher-order electric multipoles, determines sharper scattering features than what commonly available in optics, as evident by the sharp dip in Fig. 8f, which may be particularly appealing for ultrasensitive chemical and biological sensing and optical tagging, or to realize selective filters and enhanced optical bistability.

The Fano interference mechanism described in the previous paragraphs strongly boosts the magnetic response, which acquires energy from the coupling with the electric mode. Remarkably, while in all the previous experiments the magnetic resonance of nanoclusters was overshadowed by a much brighter electric response (see, e.g., Fig. 7), in the asymmetric nanoring designed in ref. 89 the magnetic dipole moment represents, around its resonance frequency, the dominant contribution of the scattering spectrum, as clearly seen in Fig. 9a. The effects of boosted optical magnetism are not only evident in the farfield scattering cross section, but also in the near field. At the broad electric resonance (Fig. 9b, left panels), the electric and magnetic fields are relatively weak, as the energy of the plasmonic oscillations is rapidly depleted due to the large radiation loss of the electric mode; instead, at the Fano scattering dip (Fig. 9b, right panels), the electric field is drastically enhanced at the gaps and a particularly intense "magnetic hot spot" appears at the center of the ring. As evident from the results in Fig. 9, this optically-induced magnetic dipole moment

is arguably stronger and purer compared to the response of other magnetic meta-molecules. The strongly enhanced and localized magnetic near field may be exploited for magnetic-based biosensors or to enhance and detect weak magnetic light-matter interactions.[103,104]

The level of interaction between electric and magnetic modes can be controlled, to a certain degree, by the amount of symmetry breaking introduced in the geometry, which may lead to optimizing the level of artificial magnetism achievable in the visible range, or even dynamically tune it. The interference of electric and magnetic modes may be described as the result of the bianisotropy introduced by an asymmetric meta-molecule.[78] In fact, when the symmetry is broken, a magneto-electric polarizability α_{em} is introduced, which modifies the electric and magnetic dipole moments of the nanoring as

$$\mathbf{p} = \alpha_e \mathbf{E}_{loc} - \alpha_{em}\eta_0\hat{\mathbf{n}} \times \mathbf{H}_{loc}$$
$$\mathbf{m} = \alpha_m \mathbf{H}_{loc} - \alpha_{em}\frac{\hat{\mathbf{n}} \times \mathbf{E}_{loc}}{\eta_0}, \quad (7)$$

where η_0 is the impedance of free space and $\hat{\mathbf{n}}$ is the unit vector normal to $\mathbf{E}_{loc}$ and $\mathbf{H}_{loc}$ [eqn (7) may be also extended to tensorial polarizabilities in the most general case]. This anisotropy implies that the magnetic dipole moment of the nanoring may be effectively enhanced by the coupling with the local electric field, consistent with the previous discussion, while at the same time the electric dipole response may be suppressed. The polarizabilities α_e, α_m and α_{em} of the asymmetric nanoring can be obtained analytically by considering different illuminations, extending the approach presented in ref. 46 and 47 for the analysis of symmetric rings. In particular, it can be shown that, by exciting the structure with a linear combination of transverse-electric and transverse-magnetic spherical harmonics, we may be able to uniquely extract the four elements of the polarizability tensor (with off-diagonal terms $\alpha_{em} = \alpha_{me}$, for reciprocal meta-molecules). Once all the polarizabilities are known, the permittivity and permeability of a metamaterial made of these bianisotropic inclusions can be readily obtained, e.g., using the homogenization formulas presented in ref. 78.

As noted in ref. 89, the response of the nanoring appears to be sensitive to perturbations along the direction of the incident electric field, especially modifications of the interparticle gaps. To better appreciate this fact, we show in Fig. 10a the evolution of the electric and magnetic scattering as a function of the displacement of one NP.[105] These results are calculated assuming plane wave illumination, and the response of the asymmetric nanoring is obtained with a dynamic dipolar analysis, which involves numerically solving a system of N equations to find the dipole moments of the individual particles. The results show that, when the particle is shifted inward (i.e., capacitive coupling is increased), the electric resonance splits and the narrower magnetic response is boosted at the dip location; conversely, outward displacements have almost negligible effect. Rather surprisingly, the magnetic response is stronger for smaller, more compact, meta-molecules. Finally, Fig. 10b highlights the extreme scenario in which the magnetic response is ideally pure, as the electric resonance has been
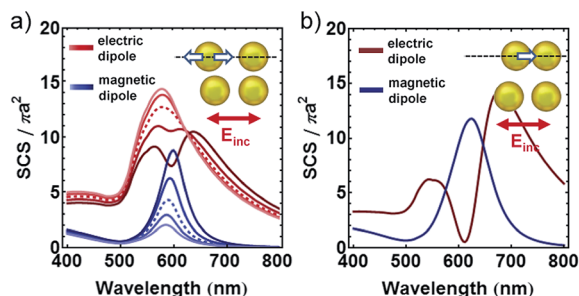
9068 | J. Mater. Chem. C, 2014, 2, 9059–9072

This journal is © The Royal Society of Chemistry 2014

Fig. 10 (a) Evolution of the electric (red lines) and magnetic (blue) scattering response, as a function of the displacement of one NP along the direction of the incident electric field, as shown in the inset. The symmetric case is shown with dashed lines. Darker (lighter) colors indicate displacement toward (away from) the neighboring particle. Reproduced with permission from ref. 105. (b) Extreme scenario in which the electric response is completely suppressed, while the magnetic moment is maximally boosted.

suppressed by the interference mechanism described in (7). This remarkable result suggests that it may be possible to create a pure local magnetic response in the visible range, with interesting implications to enhance light-matter interactions with localized magnetic emitters.[103,104]

Although the optical magnetic field usually plays just an "auxiliary" role in the interaction of light with natural materials, the findings presented here show that the fundamental asymmetry between electric and magnetic responses in the optical range does not always hold in suitably engineered magnetic meta-molecules.

5. Conclusions and outlook

In this feature article, we have discussed the recent progress in the quest to realize artificial magnetic materials, examining the associated challenges and difficulties, particularly at optical frequencies. We have shown that, although nature seems to have an aversion toward strong optical magnetism, a significant magnetic response can be attained above the THz range by relying on the displacement current, properly guided and tailored in metallic or dielectric nanostructures. In this context, plasmonic nanorings and nanoclusters, composed of NPs close to their plasmon resonance, have been shown to be particularly promising to realize artificial magnetism in the infrared and visible region. The magnetic nature of the response of these plasmonic meta-molecules is demonstrated by the consistently high level of agreement between experiments, analytical calculations and numerical simulations, as well as by the polarization- and angle-resolved scattering measurements reported in several papers (*e.g.*, ref. 82 and 84). Furthermore, we have shown that the magnetic response of plasmonic nanoclusters may be further boosted through suitable symmetry breaking that triggers dramatic Fano interference effects. Thanks to their subwavelength size, these meta-molecules seem ideal to realize optical metamaterials with negative effective permeability and negative index of refraction. Moreover, magnetic inclusions may find

application in the growing field of metasurfaces, namely, the planarized version of metamaterials, since their typical efficiency issues[106,107] may be tackled by suitably tailoring both electric and magnetic transverse currents on the surface.[108,109]

Several challenges, however, still need to be tackled before these ideas may have a real technological impact. In particular, the fabrication of large-volume three-dimensional magnetic metamaterials working at optical frequencies still represents an open research problem.[110] For example, the nanoclusters discussed in Sections 3 and 4, are generally very sensitive to geometrical perturbations and, while AFM nanomanipulation offers a large level of positional control, alternative techniques may be investigated to improve the geometrical replicability of these meta-molecules, very important to realize large arrays and metamaterials. This may be particularly challenging, as the spacing between NPs generally needs to be small (in the order of a few nanometers) to achieve the strong response and Fano resonances discussed in the previous sections. The precise control of these gaps, which determine the level of interaction between magnetic and electric modes, as discussed above, may be achieved by creating spacer layers, or with self-assembly techniques using different capping molecules.[111] Moreover, for gaps smaller than one nanometer, non-local and quantum effects may become important, opening new intriguing possibilities. As an alternative to bottom-up fabrication by AFM manipulation or self-assembly, if the spherical nanoparticles are substituted by nanodisks or nanocylinders, top-down fabrication processes can also be employed, *e.g.*, electron beam lithography, as in ref. 83. Other interesting research directions involve the investigation of different materials and heterogeneous nanoclusters. For example, the high-frequency plasmonic properties of aluminum may be used to push artificial magnetism and negative-permeability metamaterials up to the UV range. In addition, we are currently investigating how rings of dielectric NPs with high refractive index (*e.g.*, silicon) may be used to realize enhanced artificial magnetism and sharp magneto-electric Fano resonances in the visible range, with the important advantage of low absorption in dielectric materials.

All these exciting challenges and open research directions can be tackled and pursued only through a largely interdisciplinary effort, in which chemistry and material science play a fundamental role, as the emphasis is more and more on materials and structures at the nanoscale. The rise of optical metamaterial concepts and advanced nanotechnology are fulfilling the famous prediction of Richard Feynman that "when we have some control of the arrangement of things in the small scale, we will get an enormously greater range of possible properties that substances can have".[112] The artificial optical magnetism discussed in this paper represents a quintessential example of how new fundamental material properties, previously thought to be strictly unavailable, can truly be realized by the engineered arrangement of elements at the nanoscale. In this sense, the field of optical metamaterials, through the interaction between different disciplines, may be a real "game changer" in the coming years, and open exciting and uncharted directions of science and technology.

This journal is © The Royal Society of Chemistry 2014

J. Mater. Chem. C, 2014, **2**, 9059–9072 | **9069**

Acknowledgements

References

1 T. Datta, *Lett. Nuovo Cimento*, 1983, **37**, 51–54.

2 J. Preskill, *Annu. Rev. Nucl. Part. Sci.*, 1984, **34**, 461–530.

3 R. P. Feynman, R. B. Leighton and M. Sands, *The Feynman Lectures on Physics*, Addison Wesley, Boston, 2005.

4 L. D. Landau, L. P. Pitaevskii and E. M. Lifshitz, *Electrodynamics of Continuous Media*, Butterworth-Heinemann, Oxford, second edn, 1984.

5 W. Cai and V. Shalaev, *Optical Metamaterials: Fundamentals and Applications*, Springer, 2009.

6 R. Merlin, *Proc. Natl. Acad. Sci. U. S. A.*, 2009, **106**, 1693–1698.

7 V. M. Agranovič and V. L. Ginzburg, *Spatial Dispersion in Crystal Optics and the Theory of Excitons*, Wiley-Interscience, New York, 1966.

8 S. A. Schelkunoff and H. T. Friis, *Antennas: theory and practice*, Wiley, New York, 1952.

9 J. B. Pendry, A. J. Holden, D. J. Robbins and W. J. Stewart, *IEEE Trans. Microwave Theory Tech.*, 1999, **47**, 2075–2084.

10 A. Sihvola, *Metamaterials*, 2007, **1**, 2–11.

11 F. Capolino, *Theory and Phenomena of Metamaterial*, CRC Press, 2009.

12 J. B. Pendry, *Phys. Rev. Lett.*, 2000, **85**, 3966–3969.

13 F. Bilotti, A. Alu and L. Vegni, *IEEE Trans. Antennas Propag.*, 2008, **56**, 1640–1647.

14 J. B. Pendry, D. Schurig and D. R. Smith, *Science*, 2006, **312**, 1780–1782.

15 N. Engheta and R. W. Ziolkowski, *Electromagnetic Metamaterials: Physics and Engineering Explorations*, Wiley-IEEE Press, New York, 2006.

16 D. R. Smith, W. Padilla, D. Vier, S. Nemat-Nasser and S. Schultz, *Phys. Rev. Lett.*, 2000, **84**, 4184–4187.

17 D. R. Smith, J. B. Pendry and M. C. K. Wiltshire, *Science*, 2004, **305**, 788–792.

18 V. G. Veselago, *Sov. Phys. Usp*, 1968, **10**, 509–514.

19 Interestingly, natural materials exhibiting negative refraction have been proven to exist, at least in the GHz frequency range. In fact, some exotic ferromagnetic metals, *e.g.*, from the family of colossal-magnetoresistance manganites,[19] may exhibit negative refractive index close to the ferromagnetic resonance at room temperature, when immersed in a static magnetic field.

20 A. Pimenov, A. Loidl, K. Gehrke, V. Moshnyaga and K. Samwer, *Phys. Rev. Lett.*, 2007, **98**, 197401.

21 J. Zhou, T. Koschny, M. Kafesaki, E. N. Economou, J. B. Pendry and C. M. Soukoulis, *Phys. Rev. Lett.*, 2005, **95**, 223902.

22 M. W. Klein, C. Enrich, M. Wegener, C. M. Soukoulis and S. Linden, *Opt. Lett.*, 2006, **31**, 1259.

23 T. J. Yen, W. J. Padilla, N. Fang, D. C. Vier, D. R. Smith, J. B. Pendry, D. N. Basov and X. Zhang, *Science*, 2004, **303**, 1494–1496.

24 S. Tretyakov, *Metamaterials*, 2007, **1**, 40–43.

25 S. Linden, C. Enrich, M. Wegener, J. Zhou, T. Koschny and C. M. Soukoulis, *Science*, 2004, **306**, 1351–1353.

26 C. Enrich, M. Wegener, S. Linden, S. Burger, L. Zschiedrich, F. Schmidt, J. Zhou, T. Koschny and C. Soukoulis, *Phys. Rev. Lett.*, 2005, **95**, 203901.

27 S. Zhang, W. Fan, B. Minhas, A. Frauenglass, K. Malloy and S. Brueck, *Phys. Rev. Lett.*, 2005, **94**, 037402.

28 A. Ishikawa, T. Tanaka and S. Kawata, *Phys. Rev. Lett.*, 2005, **95**, 237401.

29 T. Tomioka, S. Kubo, M. Nakagawa, M. Hoga and T. Tanaka, *Appl. Phys. Lett.*, 2013, **103**, 071104.

30 M. Wheeler, J. Aitchison and M. Mojahedi, *Phys. Rev. B: Condens. Matter Mater. Phys.*, 2005, **72**, 193103.

31 Q. Zhao, J. Zhou, F. Zhang and D. Lippens, *Mater. Today*, 2009, **12**, 60–69.

32 J. C. Ginn, I. Brener, D. W. Peters, J. R. Wendt, J. O. Stevens, P. F. Hines, L. I. Basilio, L. K. Warne, J. F. Ihlefeld, P. G. Clem and M. B. Sinclair, *Phys. Rev. Lett.*, 2012, **108**, 097402.

33 A. I. Kuznetsov, A. E. Miroshnichenko, Y. H. Fu, J. Zhang and B. Luk'yanchuk, *Sci. Rep.*, 2012, **2**, 492.

34 G. Shvets and Y. A. Urzhumov, *Phys. Rev. Lett.*, 2004, **93**, 243902.

35 G. Shvets and Y. A. Urzhumov, *J. Opt. A: Pure Appl. Opt.*, 2005, **7**, S23–S31.

36 Y. A. Urzhumov and G. Shvets, *Solid State Commun.*, 2008, **146**, 208–220.

37 S. O'Brien and J. B. Pendry, *J. Phys.: Condens. Matter*, 2002, **14**, 4035–4044.

38 K. C. Huang, M. L. Povinelli and J. D. Joannopoulos, *Appl. Phys. Lett.*, 2004, **85**, 543.

39 M. L. Povinelli, S. G. Johnson, J. D. Joannopoulos and J. B. Pendry, *Appl. Phys. Lett.*, 2003, **82**, 1069.

40 S. O'Brien, D. McPeake, S. Ramakrishna and J. Pendry, *Phys. Rev. B: Condens. Matter Mater. Phys.*, 2004, **69**, 241101.

41 V. Podolskiy, A. Sarychev and V. Shalaev, *J. Nonlinear Opt. Phys. Mater.*, 2002, **11**, 65–74.

42 G. Dolling, C. Enrich, M. Wegener, J. F. Zhou, C. M. Soukoulis and S. Linden, *Opt. Lett.*, 2005, **30**, 3198.

43 J. Zhou, L. Zhang, G. Tuttle, T. Koschny and C. Soukoulis, *Phys. Rev. B: Condens. Matter Mater. Phys.*, 2006, **73**, 041101.

44 V. M. Shalaev, W. Cai, U. K. Chettiar, H.-K. Yuan, A. K. Sarychev, V. P. Drachev and A. V. Kildishev, *Opt. Lett.*, 2005, **30**, 3356.

45 W. Cai, U. K. Chettiar, H.-K. Yuan, V. C. de Silva, A. V. Kildishev, V. P. Drachev and V. M. Shalaev, *Opt. Express*, 2007, **15**, 3333.

46 A. Alù, A. Salandrino and N. Engheta, *Opt. Express*, 2006, **14**, 1557.

47 A. Alù and N. Engheta, *Phys. Rev. B: Condens. Matter Mater. Phys.*, 2008, **78**, 085112.

48 A. Alu and N. Engheta, *Opt. Express*, 2009, **17**, 5723.

49 Y. A. Urzhumov, G. Shvets, J. A. Fan, F. Capasso, D. Brandl and P. Nordlander, *Opt. Express*, 2007, **15**, 14129.

50 Q. Wu and W. Park, *Appl. Phys. Lett.*, 2008, **92**, 153114.

51 J. Valentine, S. Zhang, T. Zentgraf, E. Ulin-Avila, D. A. Genov, G. Bartal and X. Zhang, *Nature*, 2008, **455**, 376–379.

52 J. Valentine, S. Zhang, T. Zentgraf and X. Zhang, *Proc. IEEE*, 2011, **99**, 1682–1690.

53 V. M. Shalaev, *Nat. Photonics*, 2007, **1**, 41–48.

54 F. Monticone and A. Alù, *Chin. Phys. B*, 2014, **23**, 047809.

55 S. A. Maier, *Plasmonics: Fundamentals and Applications*, Springer, Berlin, 2007.

56 C. Argyropoulos, F. Monticone, G. D'Aguanno and A. Alù, *Appl. Phys. Lett.*, 2013, **103**, 143113.

57 M. W. Knight, L. Liu, Y. Wang, L. Brown, S. Mukherjee, N. S. King, H. O. Everitt, P. Nordlander and N. J. Halas, *Nano Lett.*, 2012, **12**, 6000–6004.

58 P. R. West, S. Ishii, G. V. Naik, N. K. Emani, V. M. Shalaev and A. Boltasseva, *Laser Photonics Rev.*, 2010, **4**, 795–808.

59 A. Boltasseva and H. A. Atwater, *Science*, 2011, **331**, 290–291.

60 B. Luk'yanchuk, N. I. Zheludev, S. A. Maier, N. J. Halas, P. Nordlander, H. Giessen and C. T. Chong, *Nat. Mater.*, 2010, **9**, 707–715.

61 F. Monticone, C. Argyropoulos and A. Alù, *Phys. Rev. Lett.*, 2013, **110**, 113901.

62 F. Monticone, C. Argyropoulos and A. Alù, *Sci. Rep.*, 2012, **2**, 912.

63 S. Zhang, D. A. Genov, Y. Wang, M. Liu and X. Zhang, *Phys. Rev. Lett.*, 2008, **101**, 047401.

64 F. Monticone and A. Alù, *Phys. Rev. Lett.*, 2014, **112**, 213903.

65 M. G. Silveirinha, *Phys. Rev. A*, 2014, **89**, 023813.

66 A. Alù and N. Engheta, *Phys. Rev. E: Stat., Nonlinear, Soft Matter Phys.*, 2005, **72**, 16623.

67 F. Monticone and A. Alù, *Phys. Rev. X*, 2013, **3**, 041005.

68 C. Argyropoulos, P.-Y. Chen, F. Monticone, G. D'Aguanno and A. Alù, *Phys. Rev. Lett.*, 2012, **108**, 263905.

69 M. Agio and A. Alù, *Optical Antennas*, Cambridge University Press, Cambridge, 2013.

70 C. F. Bohren and D. R. Huffman, *Absorption and Scattering of Light by Small Particles*, John Wiley & Sons, New York, 2008.

71 P. Y. Chen, F. Monticone, C. Argyropoulos and A. Alù, Plasmonic Optical Nanoantennas, in Modern Plasmonics, ed. A. Maradudin, J. R. Sambles and W. L. Barnes, Elsevier, 2014, ch. 4, pp. 109–136.

72 N. Engheta, A. Salandrino and A. Alù, *Phys. Rev. Lett.*, 2005, **95**, 095504.

73 J. Shi, F. Monticone, S. Elias, Y. Wu, D. Ratchford, X. Li and A. Alù, *Nat. Commun.*, 2014, **5**, 3896.

74 A. Alù and N. Engheta, *Phys. Rev. Lett.*, 2010, **104**, 213902.

75 N. Engheta, *Science*, 2007, **317**, 1698–1702.

76 M. Hentschel, J. Dorfmüller, H. Giessen, S. Jäger, A. M. Kern, K. Braun, D. Zhang and A. J. Meixner, *Beilstein J. Nanotechnol.*, 2013, **4**, 57–65.

77 A. H. Sihvola, *Electromagnetic Mixing Formulas and Applications*, IEE, London, 1999.

78 A. Alù, *Phys. Rev. B: Condens. Matter Mater. Phys.*, 2011, **84**, 075153.

79 J. Baena, L. Jelinek and R. Marqués, *Phys. Rev. B: Condens. Matter Mater. Phys.*, 2007, **76**, 245115.

80 C. R. Simovski and S. A. Tretyakov, *Phys. Rev. B: Condens. Matter Mater. Phys.*, 2009, **79**, 045111.

81 A. Vallecchi, M. Albani and F. Capolino, *Opt. Express*, 2011, **19**, 2754–2772.

82 S. N. Sheikholeslami, H. Alaeian, A. L. Koh and J. A. Dionne, *Nano Lett.*, 2013, **13**, 4137–4141.

83 M. Hentschel, M. Saliba, R. Vogelgesang, H. Giessen, A. P. Alivisatos and N. Liu, *Nano Lett.*, 2010, **10**, 2721–2726.

84 J. A. Fan, C. Wu, K. Bao, J. Bao, R. Bardhan, N. J. Halas, V. N. Manoharan, P. Nordlander, G. Shvets and F. Capasso, *Science*, 2010, **328**, 1135–1138.

85 J. A. Fan, K. Bao, C. Wu, J. Bao, R. Bardhan, N. J. Halas, V. N. Manoharan, G. Shvets, P. Nordlander and F. Capasso, *Nano Lett.*, 2010, **10**, 4680–4685.

86 J. A. Fan, Y. He, K. Bao, C. Wu, J. Bao, N. B. Schade, V. N. Manoharan, G. Shvets, P. Nordlander, D. R. Liu and F. Capasso, *Nano Lett.*, 2011, **11**, 4859–4864.

87 T. Junno, K. Deppert, L. Montelius and L. Samuelson, *Appl. Phys. Lett.*, 1995, **66**, 3627.

88 S. Kim, F. Shafiei, D. Ratchford and X. Li, *Nanotechnology*, 2011, **22**, 115301.

89 F. Shafiei, F. Monticone, K. Q. Le, X.-X. Liu, T. Hartsfield, A. Alù and X. Li, *Nat. Nanotechnol.*, 2013, **8**, 95–99.

90 C. N. R. Rao, G. U. Kulkarni, P. J. Thomas and P. P. Edwards, *Chem. Soc. Rev.*, 2000, **29**, 27–35.

91 S. Oldenburg, R. Averitt, S. Westcott and N. Halas, *Chem. Phys. Lett.*, 1998, **288**, 243–247.

92 E. Prodan, C. Radloff, N. J. Halas and P. Nordlander, *Science*, 2003, **302**, 419–422.

93 P. Nordlander, C. Oubre, E. Prodan, K. Li and M. I. Stockman, *Nano Lett.*, 2004, **4**, 899–903.

94 E. Prodan and P. Nordlander, *J. Chem. Phys.*, 2004, **120**, 5444–5454.

95 V. Myroshnychenko, J. Rodríguez-Fernández, I. Pastoriza-Santos, A. M. Funston, C. Novo, P. Mulvaney, L. M. Liz-Marzán and F. J. García de Abajo, *Chem. Soc. Rev.*, 2008, **37**, 1792–1805.

96 A. E. Miroshnichenko, S. Flach and Y. S. Kivshar, *Rev. Mod. Phys.*, 2010, **82**, 2257–2298.

97 M. I. Stockman, *Nature*, 2010, **467**, 541–542.

98 Capping molecules on the surface of the particles prevent them from physically touching, determining interparticle gaps in the order of the nanometer. Elsewhere[110] capping molecules have also been systematically employed to control the separation between plasmonic elements.

99 R. L. Carter, *Molecular Symmetry and Group Theory*, Wiley, New York, 1998.

100 S. N. Sheikholeslami, A. García-Etxarri and J. A. Dionne, *Nano Lett.*, 2011, **11**, 3927–3934.

101 F. Monticone and A. Alù, *Opt. Photonics News*, 2013, **24**, 35.

102 P. Nordlander, *Nat. Nanotechnol.*, 2013, **8**, 76–77.

103 S. Karaveli and R. Zia, *Phys. Rev. Lett.*, 2011, **106**, 193004.

This journal is © The Royal Society of Chemistry 2014

J. Mater. Chem. C, 2014, **2**, 9059–9072 | 9071

104 T. H. Taminiau, S. Karaveli, N. F. van Hulst and R. Zia, *Nat. Commun.*, 2012, **3**, 979.
105 F. Monticone, A. Alu and X. Li, in *2013 IEEE Antennas and Propagation Society International Symposium*, IEEE, 2013, pp. 492–493.
106 F. Monticone, N. M. Estakhri and A. Alù, *Phys. Rev. Lett.*, 2013, **110**, 203903.
107 A. Alù, *Physics*, 2013, **6**, 53.
108 C. Pfeiffer and A. Grbic, *Phys. Rev. Lett.*, 2013, **110**, 197401.
109 M. Selvanayagam and G. V. Eleftheriades, *Opt. Express*, 2013, **21**, 14409.
110 C. M. Soukoulis and M. Wegener, *Nat. Photonics*, 2011, **5**, 523–530.
111 C. Ciracì, R. T. Hill, J. J. Mock, Y. Urzhumov, A. I. Fernández-Domínguez, S. A. Maier, J. B. Pendry, A. Chilkoti and D. R. Smith, *Science*, 2012, **337**, 1072–1074.
112 R. P. Feynman, *Eng. Sci.*, 1960, **23**, 22–36.